Department of Electrical Engineering

Victor Croisfelt Rodrigues

Spatial Correlation and Low Complexity Signal Processing Techniques in Massive MIMO Systems

Final year project presented to the Department of Electrical Engineering at Universidade Estadual de Londrina (UEL) as a requirement for the conclusion of the Bachelor of Electrical Engineering (BE) honours degree.

Londrina, Brazil
2018

Universidade Estadual de Londrina

Victor Croisfelt Rodrigues

Spatial Correlation and Low Complexity Signal Processing Techniques in Massive MIMO Systems

Final year project presented to the Department of Electrical Engineering at Universidade Estadual de Londrina (UEL) as a requirement for the conclusion of the Bachelor of Electrical Engineering (BE) honours degree.

Area: Telecommunication Systems

Supervisor:
Dr. Taufik Abrão

Co-Supervisor:
Dr. José Carlos Marinello Filho

Londrina, Brazil
2018

Catalog Record

Croisfelt Rodrigues, Victor

Spatial Correlation and Low Complexity Signal Processing Techniques in Massive MIMO Systems. Londrina, Brazil, 2018. 22 p.

Final year project – Universidade Estadual de Londrina, PR. Department of Electrical Engineering.

I.Massive MIMO. II.Mitigation of Pilot Contamination. III.Spatial Correlation. IV.Low Complexity Signal Processing Techniques. V.Kaczmarz Algorithm.
Department of Electrical Engineering

Victor Croisfelt Rodrigues

Spatial Correlation and Low Complexity Signal Processing Techniques in Massive MIMO Systems

Final year project presented to the Department of Electrical Engineering at Universidade Estadual de Londrina (UEL) as a requirement for the conclusion of the Bachelor of Electrical Engineering (BE) honours degree.

Area: Telecommunication Systems

Examination Board

MsC. Jaime Laelson Jacob
Department of Electrical Engineering (UEL)
Research Professor

Dr. José Carlos Marinello Filho
Department of Electrical Engineering (UEL)
Research Professor
Co-Supervisor

Dr. Taufik Abrão
Department of Electrical Engineering (UEL)
Senior Research Professor
Supervisor

December 18, 2018

Acknowledgments

This work was a great turning point in my professional career and personal life, bringing the intense experience in wireless communication research along with several other challenges and opportunities. It also represents the end of a long and enriched journey of 5 years that I have traced with the intention of acquiring the bachelor's degree in electrical engineering.

During this period, my parents, Valdivino Rodrigues Filho and Aparecida Lourença Rodrigues, were my source of motivation and support, as was my brother Vinicius Croisfelt Rodrigues. They provided the path that I needed by solving any technical difficulties and encouraging me through inspirations. I will ever be profoundly grateful for such efforts and throughout my life I desire to honor them. It is important to evidence the support of other family members who deserve thanks as well.

I would like to offer my sincerest gratitude to Dr. Taufik Abrão for his guidance over the past eight months. He introduced me the concepts behind Massive MIMO and dedicated a great amount of time discussing and reviewing the premises of this work. In addition, he offered a myriad of opportunities and shared his vast technical and personal knowledge, for which, again, I owe my deepest acknowledgment. I am also grateful to Dr. José Carlos Marinello Filho for his advice and support via discussions and reviews of this work. It was a privilege to work with them.

I am thankful to my partner, Victória Dísparo Franco, who gave me motivational fortification throughout this year. She encouraged me to pursue my dreams and to go further. Finally, I acknowledge the friends that I made during the electrical engineering course, especially to Ricardo Fujita, Nícolas Bruno Montanha Vançan, and Karina Bernardin Rosa.

Victor Croisfelt Rodrigues

Londrina, End of 2018

Abstract

One of the most promising technologies to match the current society requirements in the fifth generation (5G) of wireless communications is the massive multiple-input multiple-output (M-MIMO) system. At a first moment, this work focused to present the canonical concepts behind this technology in order to uncover its functionality and open issues related with its envisioned implementation. As a fundamental complication of this system, the pilot contamination was studied here; where a successive pilot decontamination method was duly assessed. Some drawbacks of this approach were pointed out, whereby the use of multiple pilot training phases was seen unattractive to handle with pilot contamination. Motivated by the lack of studies associated with spatial correlation over multi-antenna channels in an M-MIMO scenario, the exponential antenna array correlation model combined with large-scale fading variations over the array was analyzed for both channel hardening and favorable propagation effects; where, the normalized mean squared error (NMSE) was also deployed as an evaluation metric. Since the current interest resides on the use of different antenna array arrangements, the performance assessment of spatially correlated M-MIMO channels was carried out deploying the uniform linear array (ULA) and the uniform planar array (UPA). Generally speaking, the favorable propagation effect was found to improve with spatial correlation, wherein UPA guarantees better results. In view of the fact that favorable propagation is properly related to channel estimation, the pilot contamination was seen reduced when considering the use of the minimum mean-square error (MMSE) estimator. Instead of these positive results, channel hardening was observed to be poorly sustained in high-spatial correlation conditions. Given these points, a trade-off between the assurance of favorable propagation and channel hardening has been discussed in order to support a more realistic network design based on the studied model. Another current research interest lies in the reduction of the complexity associated with the linear signal processing techniques applicable to M-MIMO systems. With this in mind, the Kaczmarz algorithm (KA) was implemented to solve the combining/precoding problems following some recent directions found in the literature. So as to improve the rate of convergence of this iterative algorithm, a modification in the KA has been proposed, showing good results with respect to the original one.

List of Contents

Abbreviations List

Conventions and Notations

Symbols List

1 Introduction **1**

1.1 Background 1

1.2 Contributions 4

1.3 Organization 5

2 Results **6**

3 Conclusions **8**

Bibliography **10**

Appendix A – Massive MIMO System in TDD Mode: Channel Estimation and Spectral Efficiency **11**

Appendix B – An Evaluation of Successive Pilot Decontamination in Massive MIMO **20**

Appendix C – Exponential Spatial Correlation with Large-Scale Variations in Massive MIMO Channel Estimation **21**

Appendix D – Kaczmarz Precoding and Detection for Massive MIMO Systems **22**

Abbreviations List

4G	Fourth Generation
5G	Fifth Generation
BS	Base Station
CSI	Channel State Information
DL	Downlink
KA	Kaczmarz Algorithm
LS	Least-Squares
LTE	Long-Term Evolution
MIMO	Multiple-Input Multiple-Output
M-MIMO	Massive Multiple-Input Multiple-Output
MMSE	Minimum Mean-Squared Error
MR	Maximum-Ratio
RZF	Regularized Zero-Forcing
SE	Spectral Efficiency
SINR	Signal-to-Interference-Noise-Ratio
TDD	Time-Division Duplex
UE	User Equipment
UL	Uplink
ULA	Uniform Linear Array
UPA	Uniform Planar Array
ZF	Zero-Forcing

Conventions and Notations

The following mathematical notations where adopted in this work:

	Boldface lower case letters represent vectors;
	Boldface upper case letters denote matrices;
$(\cdot)^{-1}$	Inversion operator;
$(\cdot)^{\mathrm{H}}$	Hermitian operator (transposition and conjugation);
$(\cdot)^{\mathrm{T}}$	Transposition operator;
$(\cdot)^{*}$	Complex conjugate operator;
$[\cdot,\cdot]$	Concatenation operation;
$\mathrm{diag}(\cdot)$	Diagonalization operation;
$\mathrm{tr}\,(\cdot)$	Trace operation;
$\|\cdot\|_n$	Norm of order n;
$\|\cdot\|_{\mathrm{F}}$	Frobenius norm;
$\langle\cdot,\cdot\rangle$	Inner product;
$\otimes$	Kronecker product;
$\mathbf{I}_m$	Identity matrix of order m;
$\mathbf{0}_{m\times n}$	Matrix comprised of zero elements of size $m \times n$;
$\mathbf{1}_{m\times n}$	Matrix comprised of one elements of size $m \times n$;
$\mathcal{N}_{\mathbb{C}}(\mu,\sigma^2)$	Circularly-symmetric normal distribution with mean μ and variance σ^2;
$\mathcal{O}(\cdot)$	Complexity order of an operation or algorithm;
$\mathbb{E}\{\cdot\}$	Statistical Expectation;

$\mathbb{V}\{\cdot\}$	Statistical Variance;
$\mathbb{R}$	Real numbers set;
$\mathbb{C}$	Complex numbers set;
$\in$	Belongs to the set.

Symbols List

Some symbols used recurrently in this work are defined as follows:

τ_{c}	Coherence interval;
B_{c}	Coherence bandwidth;
T_{c}	Coherence time;
τ_{p}	Pilot length;
L	Number of cells;
M	Number of BS antennas;
K	Number of UEs;
$\mathbf{g}_{jlk}$	Wireless channel linking BS j to UE k at cell l;
β_{jlk}	Average large-scale fading coefficient of UE k within cell l to BS j;
$\mathbf{h}_{jlk}$	Small-scale fading component of UE k within cell l to BS j;
$\mathbf{R}_{jlk}$	Covariance matrix of UE k within cell l to BS j;
$\mathbf{Y}_{j}^{\mathrm{p}}$	Received pilot signal matrix at cell j;
ρ^{p}	Normalized pilot training transmit power;
ρ^{ul}	Normalized UL transmit power;
$\boldsymbol{\phi}_k$	Pilot assigned to the kth UE;
$\mathbf{N}_{j}^{\mathrm{p}}$	Receiver noise matrix at cell j;
$\mathbf{y}'^{\mathrm{p}}_{ji}$	De-spreading signal for the ith UE at cell j;
$\hat{\mathbf{g}}_{jlk}$	Estimate of $\mathbf{g}_{jlk}$;
ψ_{jlk}	Average variance of $\hat{\mathbf{g}}_{jlk}$;
$\mathbf{y}_j$	Received signal in BS j in the UL phase;
s_{lk}	Information symbol transmitted by UE k within cell l;

$\mathbf{n}_j$	Receiver noise vector;
$\mathbf{v}_{jk}$	Receive combining vector of UE k within cell j;
$\mathbf{V}_j$	Receive combining matrix of BS j;
$\mathrm{SE}_{jk}^{\mathrm{ul}}$	UL SE for the kth UE attached to BS j;
$\gamma_{jk}^{\mathrm{ul}}$	SINR for the UL of UE k at cell j;
$\mathbf{x}_l$	Precoding process of cell l;
ς_{lk}	Message signal sent by BS l towards UE k;
$\mathbf{y}_{jk}$	Received signal in UE k attached to BS j in the DL phase;
$\mathbf{w}_{jk}$	Transmit precoding vector of UE k within cell j;
$\mathbf{W}_j$	Transmit precoding matrix of BS j;
$\mathrm{SE}_{jk}^{\mathrm{dl}}$	DL SE for the kth UE attached to BS j;
$\gamma_{jk}^{\mathrm{dl}}$	SINR for the DL of UE k at cell j.

1 Introduction

Given the cultural need of information exchange, the increasing presence of the wireless communication systems in the current human society is undeniable. The exponential growth trend of data rates and the number of devices, along with the requirements for a bunch of new applications, are compelling the researches to seek for new technological possibilities. The prevailing interest of these advancements is to establish the 5G of wireless networks, in order to start its operation by 2020. According to several reports provided by Cisco, this year represents the lack of the present generation, the fourth generation (4G), ruled by long-term evolution (LTE) system in sustain the enormous expected demand (ANDREWS et al., 2014). One can be pointed out that this current state-of-art type of network is achieving its maturity, where only small gains can be gathered so far. The 5G is emerging with the challenging task of providing an ubiquitous and reliable system with a high spectral efficiency (SE) associated to a rational use of the energy. In addition to these, several changes in the physical and commercial implementation of the radios are envisioned to occur, where the homogenization between the existing technologies and the new ones are also desirable to be provided. As a way to meet these requirements, M-MIMO has been consolidated as a key proposal founded on the evolution of the MIMO concept. In fact, the spatial characterization of the numerous quantity of user equipment (UE) and the huge scale of the array size at the base stations (BSs) support a vast coverage-throughput enhancement; being both features provided by M-MIMO. Besides, this approach opens the opportunities to optimize its functionality and to ponder its implementation manner. Motivated by the given scenario, this work introduces some appealing assessments and problems aiming the proper operation of the M-MIMO system.

1.1 Background

The cellular network is the most accepted way to provide the wireless services in a desired coverage area. In fact, this concept relies on split into cells the given

locality, where each cell is comprised of a BS that assures the communication between a UE and the network. With this in mind, an evident way to reach the aforementioned wanted improvement in data rates is to increase the area throughput of the cells (BJÖRNSON; HOYDIS; SANGUINETTI, 2018). This can be done through the interaction of three main components: bandwidth, cell density, and SE. One can clearly conceive that as more bandwidth a cellular network shares, better is its throughput. However, it is worth saying that the spectrum is a scarce resource and its unconcerned enlargement is physically inviable. By considering the cell density, a raise in the number of BSs per area turns the BSs closer to the UEs. This is evidently conducive to communication, but also contributes to inter-cell interference; while making network operationalization more complex and expensive. The last way embraces the improvement of SE, which strives to handle more efficiently with bandwidth and BSs pre-fixed. The employed technology in BSs is exceedingly associated with the SE enhancement and here is where the cited gains provide by M-MIMO come in.

By relying on space-division multiple access (SDMA) and the large number of antennas at the BSs, M-MIMO systems offer excellent scalability for the SE (LARSSON et al., 2014). Eventually, the UEs exploit concurrently the same time-frequency resources to communicate, which such procedure entails a multiplexing gain. These UEs are then distinguished on BS side by their respective spatial signature. However, notice that the simultaneously activities of the UEs support a nasty interference. To alleviate this undesirable effect, the BS antennas are set greater than the number of UEs within a given cell. This means that the UEs can be discriminated appropriately in BSs, since more degrees of freedoms are available to make such distinction. Also, the signals received/transmitted at each BS antenna can be coherently processed to improve the overall power of the signal. In summary, M-MIMO plays with SDMA and BS antennas to reach a desirable and superior SE bound. This gain comes with a cost since the BSs have to obtain the spatial knowledge of the UEs. One should bear in mind that the spatial signature is related to the channel response of a UE at a given communication instant.

To estimate the channel state information (CSI), M-MIMO conventionally adopts a time-division duplex (TDD) architecture. In this mode, the UEs transmit predefined pilot sequences to their respective BS; in such a way the BS roughly calculates the CSI for each UE of interest. This uplink (UL) communication period is often called as the pilot training phase. Then, by resorting to the fundamental assumption of channel reciprocity of the TDD operation, the information

acquired on pilot training also holds for the downlink (DL) period. Intending to achieve a high quality CSI, the UEs should be assigned with mutual orthogonal pilots. However, the length of pilot signaling is constrained in time and frequency due to the UE's mobility, and it also carries an undesirable overhead proportional to the number of UEs. In fact, the pilot sequences should be reused by the UEs so as to reduce the overhead and to deal with high-mobility scenarios. A common practice in literature is to reuse the pilots across different cells, while UEs within the same cell are always mutually assigned with orthogonal pilots (MARZETTA et al., 2016). This reutilization potentially introduces interference in CSI acquisition, the so-called *pilot contamination*. The main consequences of this latter effect to the system are: a) the worst quality of the channel estimation process and b) the correlation between the estimated channels of UEs assigned with the same pilot.

The massive number of BS antennas more advantageously support the benefits from the multi-antenna channels. Starting with *channel hardening* as a consequence of the spatial diversity, its effect turns the random behavior of small-scale fading into a deterministic quantity. Although conventional MIMO system usually provides this result, M-MIMO extremely magnifies the channel hardening. Another important property of multi-antenna channel is the *favorable propagation*. This feature says that the channels between UEs tend to orthogonality, as a consequence of the aforesaid spatial degrees of freedom afforded by the BS antennas. Recall that once the channel of interfering UEs are said gradually orthogonal in SDMA, their interference tends to be negligible. It is important to stress that these given properties are dependent of spatial correlation and antenna arrangement. In M-MIMO, *spatial correlation* arises from the large number of antennas be agglomerated within a confined space, and also from the propagation medium arrangement. The *antenna arrays* of the BSs can exhibit several characteristics, the most important being their shapes and sizes. Particularly, the ULA and UPA are the most common adopted array arrangements (BJÖRNSON; HOYDIS; SANGUINETTI, 2018). One needs to keep in mind that each antenna array differently affects the communication.

Despite of the fact that the non-linear signal processing schemes are conceived as the optimal to coherently process the received/transmitted signals on BS antennas, M-MIMO sufficiently reduces the interference level of SDMA to get *linear signal processing techniques* nearly optimal (BJÖRNSON; HOYDIS; SANGUINETTI, 2018). This is a direct consequence of favorable propagation and desirable from the standpoint of computational complexity. Recall that linear signal processing

schemes rely on CSI to be computed; in addition, these techniques control the SE boundary.

1.2 Contributions

As a first analysis, we describe a canonical M-MIMO system operating in TDD mode and adopting an MMSE estimator to estimate the channel responses. This system is then evaluated in terms of channel estimation and SE metrics. The pilot contamination effect is duly observed and identified as a limit of M-MIMO operation. For the purpose of mitigate pilot contamination, the study of successive pilot decontamination methods is conducted, where a set of multiple phases of pilot training is utilized (VU; VU; QUEK, 2014). Eventually, the latter techniques are found impractical due to their numerous disadvantages.

Motivated by the recent and promising studies of spatial correlation effects in M-MIMO[1], the exponential correlation model under ULA and UPA arrangements and with large-scale fading variations over the array is analyzed. The exponential correlation model is a single-parameter model that describes well the spatial correlation that arises from the proximity between the antenna elements of an array (LOYKA, 2001). Moreover, the unequal contribution of each antenna on the array is supported by channel measurements and, therefore, represents a more realistic condition (GAO et al., 2015). It is observed the impacts of each antenna array adopting such spatial correlation model over the channel hardening and favorable propagation effects. This analysis corroborates the reference results provided by the spatially uncorrelated scenario. In summary, it is found that the spatial correlation effect and array arrangement can mitigate the pilot contamination impact when adopting MMSE channel estimation. This effect shows more favorable on UPA, since this type of array achieves a higher-level of spatial correlation than the ULA counterpart. Although the pilot contamination is reduced, the channel hardening is poorly achieved for high-spatial correlation scenarios. The latter statement points to a trade-off between channel hardening and favorable propagation, which requires to be taken into account in network designs.

In spite of the fact that canonical linear signal processing techniques are of less computational complexity than non-linear ones, their computation are still

[1]For instance (BJÖRNSON; HOYDIS; SANGUINETTI, 2018), wherein the authors demonstrated that the SE in M-MIMO system does not have a fundamental limit under spatial correlation and when adopting optimal signal processing techniques.

burden; in view of their computational proportion in relation to the number of both BS antennas and UEs of a given system. This fact currently provides the seek for relaxing linear signal processing schemes to allow the employment of low complexity central nodes in networks envisioning M-MIMO adoption. With this is mind, the KA is introduced as a solution of this problem considering the zero-forcing (ZF) and regularized zero-forcing (RZF) canonical schemes, as proposed in BOROUJERDI; HAGHIGHATSHOAR; CAIRE (2018). It is important to say that the KA is an iterative solver of system of linear equations. Herein, we introduce modifications in the KA routine applied in M-MIMO (as a precoder and decoder) that lead to a better rate of convergence. Furthermore, a different application perspective is investigated in order to make feasible the computational appealing of KA-based signal processing techniques. It is worth saying that more realistic conditions are comprised in our work with respect to the original proposal[2]. This last assertion is a consequence of the utilization of both least-squares (LS) and MMSE channel estimations under uncorrelated and correlated fading circumstances.

1.3 Organization

The remainder of this monograph is structured in the form of papers, which were developed and conceived throughout the period from March to November of 2018 destined to the accomplishment of this work. The conclusions and key points of the work are given in Chapter 3.

[2]One can be highlighted that the authors in BOROUJERDI; HAGHIGHATSHOAR; CAIRE (2018) do not consider any real channel estimation procedure to demonstrate their results.

2 Results

As aforementioned in Section 1.3, the results are disposed in the conceived papers following the chronological order of development; the last described in Section 1.2. The papers are attached as appendices, being these listed as:

[A] Massive MIMO System in TDD Mode: Channel Estimation and Spectral Efficiency
Authors: Victor Croisfelt Rodrigues and Taufik Abrão.
Technical Report.

[B] An Evaluation of Successive Pilot Decontamination in Massive MIMO
Authors: Victor Croisfelt Rodrigues and Taufik Abrão.
Exact and Technological Sciences, Semina.
DOI: 10.5433/1679-0375.2018v39n2p107.

[C] Exponential Spatial Correlation with Large-Scale Fading Variations in Massive MIMO Channel Estimation
Authors: Victor Croisfelt Rodrigues, José Carlos Marinello Filho, and Taufik Abrão.
Transactions on Emerging Telecommunications Technologies (ETT), Wiley.
DOI: 10.1002/ett.3563.

[D] Kaczmarz Precoding and Detection for Massive MIMO Systems
Authors: Victor Croisfelt Rodrigues, José Carlos Marinello Filho, and Taufik Abrão.
Presented at: IEEE Wireless Communications and Networking Conference (IEEE WCNC), April, 2019.

The canonical M-MIMO study along with its evaluation via channel estimation and SE metrics is presented in [A]. This work adopts the MMSE channel estimation procedure realized in TDD mode under uncorrelated Rayleigh fading. Besides, it embraces the application of maximum ratio (MR) combining/precoding and ZF linear processing techniques on UL and DL phases. Some illustrative

results are carried out to present the performance of the MMSE estimator and the gains provided by both BS antennas and SDMA.

The pilot contamination impact is easily seen when comparing the system performance with an M-MIMO equivalent system only affected by receiver noise. Then, a successive pilot contamination mitigation strategy is discussed in [B]. This technique is based on the realization of multiple pilot training phases and shown several drawbacks that is duly indicated in such work.

Subsequently, the compound of exponential spatial correlation with large-scale fading variations over the array is described in [C]. Recall that this study evaluates the channel hardening and favorable propagation effects for ULA and UPA arrangements. Also, the MMSE channel estimation is assessed in order to observe the pilot contamination behavior under the consideration of spatial correlation and different types of antenna arrays.

Last, the KA-based linear processing schemes for ZF and RZF are investigated in [D], wherein a proposal of our authorship is introduced to improve the KA's rate of convergence. The SE evaluation metric is used in this work when applying LS and MMSE channel estimation procedures along with uncorrelated and correlated fading scenarios.

3 Conclusions

This monograph comprises the study of several concepts and open issues of M-MIMO. This conclusion section is composed by the conclusion contents established in the papers [A], [B], [C] and [D]. Generally speaking, several topics related to M-MIMO operation are treated throughout this work, such as, pilot contamination, spatial correlation, antenna arrays, and the seek for low complexity signal processing techniques.

The canonical functionality of an M-MIMO system was duly investigated for MMSE channel estimation and for the adoption of MR and ZF transmitter/-receiver schemes. The analysis was founded on tight closed-expressions of SE supported by the use of MMSE channel estimate. It was possible to perceive the fundamental contribution between the BS antennas and SDMA to provide via M-MIMO the high-expected gain in SE for 5G. The pilot contamination was observed as a crucial limit for the M-MIMO performance. This has motivated the study of techniques to mitigate pilot contamination. One of these investigated schemes was the successive pilot decontamination method, which presents a lot of drawbacks for its practical implementation. One can be cited the difficult associated with the synchronization of the cells to perform the multiple pilot training phases.

The spatial correlation analysis embracing the composed model comprised of the exponential correlation model with large-scale fading variations over the array presented key findings to the design of networks envisioning to adopt such procedure. Besides, it was also explored results to the adoption of ULA and UPA arrangements. It was observed that UPA provides a stronger spatial correlation than ULA; such result is in-line with intuition, since the antenna elements on UPA are more spatially confined. Some gains on the MMSE channel estimation procedure were found for spatially correlated channels, whereby the pilot contamination effect was progressively mitigated as the spatial correlation level has became higher. These last conclusions are directed related to the improvement of the favorable propagation effect provided by spatial correlation. On the

other hand, the channel hardening was dramatically affected by spatial correlation, which fact gives rise to a trade-off between the two multi-antenna effects. Therefore, although high-spatial correlation assures more favorable conditions to channel estimation, it does not provide high-hardened channel effects. Striving to compensate for this poor channel hardening, the number of BS antennas can be increased; however, as more antennas the BS has, the area and the quantity of signal processing circuits increase as well. It is up to the network designer select the more appropriate condition for his application.

Once the reduction of computational complexity related to the signal processing techniques is a desired property to be achieved, the KA was applied to solve the ZF and RZF combining/precoding problems. Moreover, it was observed that the KA operation is strongly impacted by the fundamental phenomenon related to the propagation of electromagnetic waves. By relying on such finding, an alternative approach to initialize the KA was proposed. The suggested method was evaluated for LS/MMSE channel estimators under uncorrelated and correlated fading scenarios. In conclusion, our proposal demonstrated to overcome the original procedure, which is given in BOROUJERDI; HAGHIGHATSHOAR; CAIRE (2018), in all evaluated scenarios.

Bibliography

ANDREWS, J. G.; BUZZI, S.; CHOI, W.; HANLY, S.; LOZANO, A.; SOONG, A. C. K.; ZHANG, J. C. What Will 5G Be? **IEEE Journal on Selected Areas in Communications**, v. 32, n. 6, p. 1065–1082, 2014. ISSN 0733-8716.

BJÖRNSON, E.; HOYDIS, J.; SANGUINETTI, L. Massive MIMO Has Unlimited Capacity. **IEEE Transactions on Wireless Communications**, v. 17, n. 1, p. 574–590, 2018. ISSN 15361276.

BOROUJERDI, M. N.; HAGHIGHATSHOAR, S.; CAIRE, G. Low-Complexity Statistically Robust Precoder/Detector Computation for Massive MIMO Systems. **IEEE Transactions on Wireless Communications**, IEEE, p. 1–32, 2018. ISSN 15361276.

GAO, X.; EDFORS, O.; RUSEK, F.; TUFVESSON, F. Massive MIMO Performance Evaluation Based on Measured Propagation Data. **IEEE Transactions on Wireless Communications**, v. 14, n. 7, p. 3899–3911, 2015. ISSN 1536-1276.

LARSSON, E. G.; EDFORS, O.; TUFVESSON, F.; MARZETTA, T. L. Massive MIMO for Next Generation Wireless Systems. **IEEE Communications Magazine**, v. 52, n. 2, p. 186–195, 2014. ISSN 01636804.

LOYKA, S. Channel Capacity of MIMO Architecture Using the Exponential Correlation Matrix. **IEEE Communications Letters**, v. 5, n. 9, p. 369–371, 2001. ISSN 1089-7798.

MARZETTA, T. L.; LARSSON, E. G.; YANG, H.; NGO, H. Q. **Fundamentals of Massive MIMO**. Cambridge, UK: Cambridge University Press, 2016. ISBN 9781107175570.

VU, T. X.; VU, T. A.; QUEK, T. Q. S. Successive pilot contamination elimination in multiantenna multicell networks. **IEEE Wireless Communications Letters**, v. 3, n. 6, p. 617–620, 2014. ISSN 21622345.

Appendix A – Massive MIMO System in TDD Mode: Channel Estimation and Spectral Efficiency

This technical report may be useful for those who are starting to study Massive MIMO. For this reason, its simulation code, along with the PDF of this final year project, is available on:

https://github.com/victorcroisfelt/final-year-project

Massive MIMO System in TDD Mode: Channel Estimation and Spectral Efficiency

Victor Croisfelt Rodrigues, Taufik Abrão, *Senior Member, IEEE*

Technical Report

***Abstract*—Massive multiple-input multiple-output (M-MIMO) is one of the most promising technologies for the fifth generation (5G) of cellular networks. The understanding of its principles and impairments is fundamental to support its application and to make clear the possibilities associated with this technology. In this work, we describe a canonical M-MIMO system operating in a time-division duplex (TDD) mode and discuss the main concepts behind it, as channel hardening, favorable propagation, and pilot contamination. Tight closed-form expressions and illustrative results are given to support the comprehension.**

I. Introduction

Emerging demand for higher data rates, as well as the exponential growth in the number of wireless devices, has given rise to the requirement of new technologies and the debate about a 5G standard for the upcoming cellular network [1]. First conceived in [2], M-MIMO became a key of these 5G technologies, mainly thanks to its attractive potentials in enhance the spectral efficiency (SE) and reliability, consequently increasing the system capacity; also it is an enabler of energy efficiency (EE), which is a pertinent aspect from economic, environmental, and health points of view [3]. By exploiting the spatial multiplexing of the numerous user equipment (UE), M-MIMO scales up the conventional Multiuser MIMO, achieving much better performance [4]. In its basic form, M-MIMO consists of a base station (BS) equipped with a few hundred antennas, which communicates with tens single-antenna UEs over the same time-frequency resources. The UEs are conceived to concurrently employ the entire available bandwidth through space-division multiple access (SDMA). Further, M-MIMO commonly embraces a multi-carrier modulation scheme, to take advantage of its properties that mildly handle with the wireless phenomenology.

The guidelines behind M-MIMO are based on processing techniques applied coherently over the transmitted/received signals at the BS antennas. Starting with the uplink (UL), the BS has to discriminate among the data signals sent by different UEs using a receive combing strategy; by which the desired data is spatially separated from the interfering signals. Instead, a transmit precoding scheme can be used to steer data signals from distinct antennas to a desired UE in the downlink (DL), where either the power level and phase shift of each antenna can be changed in order to achieve the UE's location. Notice that such methods are supported and enhanced by the large number of antennas. First, the decoder has a lot of information that can be exploited to achieve a better rough guess about the received signal. Secondly, the precoder has a substantial increment on the available degrees of freedom, which consequently provides more ways to guide the signal towards a UE. In practice, the BS has to accurately estimate the instantaneous channel state to be benefited with such procedures, being this knowledge referred to as the channel state information (CSI) [5]. To clarify this need, observe that to recover a desired information received from a UE and to perform signal focusing, the UEs spatial signature is a crucial knowledge to be regularly known in BSs. This essentially allows the use of spatial signal processing techniques to enhance the communication quality.

Victor Croisfelt. R. and Taufik Abrão are with State University of Londrina (UEL), Electrical Engineering Department, Rodovia Celso Garcia Cid, Km 380, s/n, 86057-970, Londrina, Brazil (e-mail: victorcroisfelt@gmail.com, taufik@uel.br).

A. Time-Division Duplex Scheme

M-MIMO conventionally operates in TDD mode, where the UL and DL phases occur at different instants, but use the same frequency band for transmission. It is then possible to observe that the channel responses in both directions can be ideally considered to be the same within a short time-frequency interval. This gives rise to a consideration known as channel reciprocity. By exploiting this supposition, the CSI can be acquired in an UL transmission referred to as the pilot training, whereby the UEs send predefined pilot signals to its own BS. The BS can so estimate the UL channel response and use this information in DL. Channel reciprocity is considered a reasonable assumption in practice. However to guarantee this last feature, the transceiver chains are needed to be calibrated. This calibration is motivated due to the non-reciprocity between BSs and UEs hardwares [6]. In contrast to CSI in BS, the UEs only require to know a constant term to decode its message in the DL phase. As demonstrated in [7], this constant term can be estimated blindly on the UE side. In summary, TDD mode has been sustained as an attractive scheme to estimate the channel responses since M-MIMO inception. This adoption can be explained because of the fact that the pilot overhead is independent of the number of antennas, which is perceptively large in M-MIMO. Another property that corroborates to TDD is that it does not need to have an information feedback between the BSs and UEs.

Although of TDD be the canonical scheme, it is important to stress that some researches are striving to make M-MIMO scalable with frequency-division duplex (FDD), which is an important strategy from an economic standpoint. One can emphasize that the TDD mode has some drawbacks due

to the channel reciprocity. As for instance, the fact that the hardware has to be constantly calibrated at both sides, intending to guarantee an acceptable reciprocity assumption, as aforementioned. Moreover, the signal-to-interference-noise (SINR) ratio is slight better in the FDD scheme (around 3 dB) when compared to that obtained by TDD.

B. Coherence Interval and Resource Block

A fundamental characteristic of wireless communications is that the channel response varies over time and frequency, as a consequence of the fading nature. Hereupon, it would be attractive if somehow, the signal processing involving the estimation and payload data transmissions were performed within a time-frequency block, in which the channels can be considered approximately static. The channel estimates would be valid throughout this interval, enabling the exploitation of these informations and, consequently, the usage of spatial signal processing schemes. Fortunately, the channel effect is said to be stationary within a sample period known as a coherence interval, which embodies the concepts of both coherence time and bandwidth at a given propagation scenario. The coherence time T_{c} is the large period of time (in seconds) wherein a channel can be regarded as time-invariant. Furthermore, the coherence bandwidth B_{c} is the frequency interval (in Hertz) in which the channel response is almost constant. The coherence block is so defined as $\tau_{\mathrm{c}} = B_{\mathrm{c}}T_{\mathrm{c}}$ (in samples) and it is dependent of the propagation environment, antenna radiation pattern, UE mobility and carrier frequency [8]. Generally, the UEs have individual coherence attributes. For the sake of network design, τ_{c} is determined by the worst-case scenario of a given environment. This worst-case period is commonly defined as the resource block.

The pilot training expends a fraction of the coherence interval as an overhead, sending pilots from UEs to BS antennas and using the resultant samples to payload data transmission. Note that the number of pilots is proportional to the quantity of UEs within a cell and it is undesirable to have those UEs interfering with each other. Thus, the pilots are conceived to be mutually orthogonal between the UEs attached to the same BS. However, realize that the pilot length is constrained by the coherence interval, in which the latter is excessively limited due to high mobility scenarios and other channel impairments. It is therefore difficult to generate a sufficient number of orthogonal sequences within a short coherence interval, leading to the reuse of the pilot sequences across the cells of a given system. For this reason, the CSI estimation suffers from an inaccuracy caused by the interference generated from UEs assigned with the same pilot sequence. This phenomenon is commonly termed as the pilot contamination, being considered to constitute a fundamental limit of the M-MIMO systems [2], [9].

C. Favorable Propagation and Channel Hardening

Once the spatial signatures from different UEs are sufficiently distinct, the fully isotropic fading environment is considered as a favorable propagation medium. In this scenario, the BS is able to easily distinguish between any peer of UEs, since there is none or a slight correlation between them. Under this exclusive non-line-of-sight (NLoS) condition, the channel responses are modeled following an independent identically distributed (i.i.d.) Rayleigh distribution. Given these points, the favorable propagation effect can be defined as the ability of an environment to permit the proper distinction of the spatial characteristics between UEs. This property can be mathematically described as the asymptotic or gradual orthogonality between the channel vectors from different UEs.

Another important effect originated from employing a large number of BS antennas is the channel hardening phenomenon. This effect relies on the law of large numbers, stating that the channel gain, naturally a random variable, tends to almost achieve its expected value for a large quantity of antenna elements. In other words, the channel hardening implicates that the small-scale fading and the frequency dependence tend to vanish for a substantial number of antennas due to the spatial diversity. This last phenomenon is assured by the fact that the small-scale fading is unable to negatively impact the signal transmitted/received by each antenna across the array, simultaneously. Consequently, the resource allocation and power control algorithms in M-MIMO are merely depended on the second order moments of the channel vectors, which commonly change slowly when compared to rapid fading. Moreover, the capacity bounds derived for a M-MIMO context are prone to be more tight due to this phenomenon.

D. Linear Signal Processing Techniques

Relying on favorable propagation and channel hardening effects, linear signal processing techniques are considered to be near optimal for the payload transmission [5], [9]. In UL, the simplest choice is the maximum-ratio (MR) combining, which maximizes the power of a UE signal by applying its channel estimate [8]. The MR actually performs a coherent sum of the information received at each antenna. This results in a signal amplification, termed as an array gain, proportional to the number of antennas. Another classical method is the zero-forcing (ZF) combining. In addition to the MR, ZF seeks to eliminate the intra-cell interference among the UEs attached to the same BS.

The transmit precoding is strongly connected with the receive combining in a heuristic form, a relation referred to as UL-DL duality. So, the signal steering vectors can be obtained through linear precoding techniques based on both MR and ZF principles. Eventually, it is important to emphasize that the MR and ZF are a suboptimal type of linear signal processing. The optimal is said to be the M-MMSE decoding scheme, whereby the UL SE is maximized [8]. Underlying the UL-DL duality, this last scheme is also considered to be optimal for the precoder.

E. Content and Contributions

The goal of this work is to demonstrate the operation of a classical M-MIMO system. This is done by presenting a system model comprised of the pilot training and UL/DL payload phases. After a detailed presentation of the given points, some numerical results are obtained to illustrate the

functionality and to explain some fundamental concepts of M-MIMO.

Notations: The superscripts $^{\mathrm{T}}$ and $^{\mathrm{H}}$ denote the transpose and the Hermitian transpose, successively. The $\mathcal{N}_{\mathbb{C}}(\cdot,\cdot)$ stands for the circularly symmetric complex Gaussian distribution. The statistical operators $\mathbb{E}\{x\}$ and $\mathbb{V}\{x\}$ represent the expected value of a random variable x and its variance, respectively. The $N \times N$ identity matrix is indicated by $\mathbf{I}_N$.

II. A Canonical Multi-cell Massive MIMO System

A canonical M-MIMO system comprised of L cells is considered here. In each cell, an autonomous BS[1] is located at the cell center and equipped with an array of M antenna elements; furthermore, a set of K single-antenna UEs is served by each BS. The cells are operating synchronously, which means that the UL and DL phases are coordinated among the cells. Moreover, they are employing the same time-frequency resources to provide communication. In order to make the linear processing techniques nearly optimal, it is adopted that $M/K > 1$ and $M \gg 1$. These conditions support the channel hardening effect and the interference reduction by means of favorable propagation. The synchronous activities and equal number of UEs within each cell are only assumed to simplify the upcoming formulation and both ones could be relaxed. As a final point, our interest lies in the operation of a specific cell called as the home cell and denoted by the index j.

The cells are situated in a fully isotropic fading environment; in such a way the link between a UE to one of the antennas at BS j is considered to be static within a τ_{c}-length block and statistical independent across the blocks realizations[2]. Alternatively, it is said that the channel is flat and time-invariant, being represented simply as a multiplication by a complex-scalar gain. The $M \times 1$ vector representing the wireless channel from UE k within cell l to BS j is denoted as $\mathbf{g}_{jlk} = \sqrt{\beta_{jlk}}\mathbf{h}_{jlk}$; where $\mathbf{h}_{jlk} \in \mathbb{C}^{M\times 1}$ represents the small-scale fading with a Rayleigh distribution, $\mathbf{h}_{jlk} \sim \mathcal{N}_{\mathbb{C}}(\mathbf{0}, \mathbf{I}_M)$. Moreover, β_{jlk} is the average large-scale fading coefficient, which incorporates the macroscopic propagation phenomena that change slowly over time. Note that β_{jlk} is only related to the UEs and it is considered identical for all elements of the antenna array. In fact, the channel vector can be rewritten in a purely statistical form as $\mathbf{g}_{jlk} \sim \mathcal{N}_{\mathbb{C}}(\mathbf{0}, \beta_{jlk}\mathbf{I}_M)$, where $\beta_{jlk}\mathbf{I}_M$ is the channel covariance matrix; since the mean is the zero vector, and $\frac{1}{M}\mathrm{tr}\left(\beta_{jlk}\mathbf{I}_M\right)$ is the average large-scale fading, β_{jlk}. Henceforth, we will assume that the average large-scale coefficients are known a priori for anyone who needs to know them. Effectively, the large-scale coefficient of each UE has to be estimated similarly to the channel response vector, but this consideration is beyond the scope of this work.

[1]This work considers a outdoor scenario, wherein each BS covers an extensive-area and gives support to mobility between the cells. In this scenario, the beachfront spectrum comprised of frequencies in the range of 2-6 GHz is commonly adopted, due to its propagation features.

[2]The block-independence is not strictly necessary, but this condition highlight that M-MIMO does not use the correlation per block, even if it is existent [9].

A. Uplink Pilots and Channel Estimation

The pilot training phase comprises of all UEs in the system transmitting their τ_{p}-length pilot sequences to their respective BS. Those pilots are previously recognized at both link ends. So that the pilot contamination can be assessed, the pilots are assumed to be reused across the L cells, as a result of the difficult to generate a large number of orthogonal pilot sequences inside a short coherence interval. For ease of exposition, it is considered that $\tau_{\mathrm{p}} = K$. So, one needs to keep in mind that the ith UE through the L cells are assigned with the same pilot, otherwise the pilots are mutually orthogonal between the UEs. Thus, the intra-cell interference is negligible in the estimation phase, whereas the inter-cell disturbance considerably impacts the system performance. Additionally, one can emphasize that those pilots are assigned randomly among the UEs in each cell, indicating the usage of a classical assignment scheme available in literature [2].

The received pilot signal at the home cell is a linear combination of the transmitted pilots from all cells, yielding in the follow $M \times \tau_{\mathrm{p}}$ received pilot signal matrix:

$$\mathbf{Y}_j^{\mathrm{p}} = \sqrt{\rho^{\mathrm{p}}} \sum_{l=1}^{L} \sum_{k=1}^{K} \mathbf{g}_{jlk}\boldsymbol{\phi}_k^{\mathrm{H}} + \mathbf{N}_j^{\mathrm{p}}, \tag{1}$$

where ρ^{p} is the normalized[3] transmit power spent on pilot training and it is given by $\rho^{\mathrm{p}} = \tau_{\mathrm{p}}\rho^{\mathrm{ul}}$, being ρ^{ul} the UL normalized power; $\boldsymbol{\phi}_k \in \mathbb{C}^{\tau_{\mathrm{p}}}$ is the pilot assigned to UE k within cell l, which has zero mean and unit norm: $\|\boldsymbol{\phi}_k\|^2 = \boldsymbol{\phi}_k^{\mathrm{H}}\boldsymbol{\phi}_k = 1$. $\mathbf{N}_j^{\mathrm{p}} \in \mathbb{C}^{M\times\tau_{\mathrm{p}}}$ is the receiver noise matrix, which is modeled as an additive white Gaussian noise (AWGN) with entries distributed as $\mathcal{N}_{\mathbb{C}}(0,1)$.

Afterwards, the home cell BS successively correlates the received signals with the pilot sequences attached to each UE. This results in the following de-spreading signal for the ith UE:

$$\mathbf{y}'^{\mathrm{p}}_{ji} \triangleq \mathbf{Y}_j^{\mathrm{p}}\boldsymbol{\phi}_i = \sqrt{\rho^{\mathrm{p}}} \sum_{l=1}^{L} \mathbf{g}_{jli} + \mathbf{n}'^{\mathrm{p}}_{li}, \tag{2}$$

where $\mathbf{n}'^{\mathrm{p}}_{li} \in \mathbb{C}^M$ is an equivalent white Gaussian noise matrix with i.i.d. elements following $\mathcal{N}_{\mathbb{C}}(0,1)$. The distribution parameters are maintained due to the operation linearity, regarding on the fact that pilot has zero mean and unit norm. The de-spreading signal represents the neat observation acquired in BS j; in the sense that it is not dependent on the pilot sequences and whereby estimation techniques can be applied thereon to obtain the CSI at a given coherence block. Either, note that the linear combination with the UEs within other cells evidenced the pilot contamination effect.

The observation in (2) is utilized by BS j to estimate the channel vectors. Considering that we know some prior knowledge of the observation, as its distribution and statistical parameters, it is possible to apply a Bayesian estimation approach. This procedure leads to a more accurate guess than the classical estimation methods [10]. Since the acquired signal is following a circularly symmetric complex Gaussian distribution, the minimum mean square error (MMSE) estimator

[3]The term "normalized" signifies that the transmit power is already taking into account the noise power.

is explicitly to be obtained. Given these points, the MMSE estimation of $\mathbf{g}_{jlk}$ based on $\mathbf{y'}^{\mathrm{p}}_{jk}$ is:

$$\mathbb{E}\left\{\mathbf{g}_{jlk}|\mathbf{y'}^{\mathrm{p}}_{jk}\right\} = \hat{\mathbf{g}}_{jlk} = \frac{\sqrt{\rho^{\mathrm{p}}}\beta_{jlk}}{1+\rho^{\mathrm{p}}\sum_{l'=1}^{L}\beta_{jl'k}}\mathbf{y'}^{\mathrm{p}}_{jk}. \quad (3)$$

According to the orthogonality principle [10], the estimate, $\hat{\mathbf{g}}_{jlk}$, and the estimation error, $\tilde{\mathbf{g}}_{jlk} = \hat{\mathbf{g}}_{jlk} - \mathbf{g}_{jlk}$, are uncorrelated random vectors. This fact also implicates the independence of those quantities, since they are Gaussian distributed. Thus, they can be given out as $\hat{\mathbf{g}}_{jlk} \sim \mathcal{N}_{\mathbb{C}}(\mathbf{0}, \psi_{jlk}\mathbf{I}_M)$ and $\tilde{\mathbf{g}}_{jlk} \sim \mathcal{N}_{\mathbb{C}}(\mathbf{0}, (\beta_{jlk} - \psi_{jlk})\mathbf{I}_M)$, where the average variance of the estimate is:

$$\psi_{jlk} = \frac{\rho^{\mathrm{p}}\beta^2_{jlk}}{1+\rho^{\mathrm{p}}\sum_{l'=1}^{L}\beta_{jl'k}}. \quad (4)$$

Note that the channel estimates from UEs that are assigned with the same pilot are correlated as:

$$\mathbb{E}\left\{\hat{\mathbf{g}}_{jlk}\hat{\mathbf{g}}^{\mathrm{H}}_{jl'k}\right\} = \frac{\rho^{\mathrm{p}}\beta_{jlk}\beta_{jl'k}}{1+\rho^{\mathrm{p}}\sum_{l''=1}^{L}\beta_{jl''k}}, \quad (5)$$

whereby the BS is unable to separate the contaminating UEs, emphasizing the severe impact caused by the pilot contamination.

B. Uplink Data Transmission

During UL payload data transmission, the UEs independently transmit they data streams to their respective BS. The received $M \times 1$ baseband signal matrix at BS j is given as a linear combination of the K transmitted signals over the entire system, expressed as:

$$\mathbf{y}_j = \sqrt{\rho^{\mathrm{ul}}}\sum_{l=1}^{L}\sum_{k=1}^{K}\mathbf{g}_{jlk}s_{lk} + \mathbf{n}_j, \quad (6)$$

where $s_{lk} \sim \mathcal{N}_{\mathbb{C}}(0,1)$ is the information symbol transmitted by UE k within cell l and $\mathbf{n}_j \sim \mathcal{N}_{\mathbb{C}}(\mathbf{0}, \mathbf{I}_M)$ is the receiver noise. We consider that the information signals are Gaussian distributed, because it is a presumption that helps the derivation of both SE and channel capacity metrics; by handling the Shannon's formula. Also, in such condition, the differential entropy of the signal is maximized as demonstrated in [9]. One should note that practical systems apply different modulation schemes over the information signal. For instance, the quadrature amplitude modulation entails slight losses in performance when compared to the infinite number of constellation points provided by the Gaussian distribution usage.

The BS is capable of detect the symbol transmitted by a desired UE under application of a receive combining scheme. If this procedure is properly selected, it may be beneficed from the signal copies received by the large number of antennas, in detriment of the interfering signals and noise. Therefore, the information from UE k at BS j is discriminated by the use of a combining vector $\mathbf{v}_{jk} \in \mathbb{C}^M$, in such a way that its detected symbol is $\mathbf{v}^{\mathrm{H}}_{jk}\mathbf{y}_j$. For the receive combining, we consider the MR and ZF schemes defined as [3]:

$$\mathbf{v}^{\mathrm{H}}_{jk} = \begin{cases} \frac{1}{\sqrt{M}}\hat{\mathbf{g}}^{\mathrm{H}}_{jjk} & \text{, Maximum Ratio} \\ \left(\hat{\mathbf{g}}^{\mathrm{H}}_{jjk}\hat{\mathbf{g}}_{jjk}\right)^{-1}\hat{\mathbf{g}}^{\mathrm{H}}_{jjk} & \text{, Zero-Forcing} \end{cases}, \quad (7)$$

note that these combiners only need the channel estimate of the UEs within the evaluated cell.

The UL SE can be obtained applying a use-and-forget technique as proposed in [5], by which the receiver neglects its knowledge of the channel estimates in the signal recover. In this way, a lower bound expression is permitted to be derived, which does not rely on randomness entailed by the fading process. Thus, the achievable SE for UE k within BS j is lower bounded by,

$$\mathrm{SE}^{\mathrm{ul}}_{jk} = \frac{1}{2}\left(1 - \frac{\tau_{\mathrm{p}}}{\tau_{\mathrm{c}}}\right)\log_2\left(1+\gamma^{\mathrm{ul}}_{jk}\right), \quad (8)$$

where the pre-log factor quantifies the energy used upon the UL payload transmission withdrawing the coherence fraction spent on pilot training. Furthermore, the division by two stress that half of the coherence samples, which were not applied on pilot training, is employed to the UL phase; while the other half is spent in DL.

To compute the SE in (8), we have to obtain the effective[4] SINR, $\gamma^{\mathrm{ul}}_{jk}$, which is determined by the power computation of the combining process. As derived in [5], the effective SINR for the MR and ZF combiners are exhibited respectively in (9) and (10) (see [5] for detailed derivation).

For the matter of argument and considering complex-valued samples, the SE metric represents the average information, evaluated in number of bits, that can be dependably transmitted over a wireless link. This definition is very linked to the selected precoder/decoder and the channel modeling. In our case, the channel is modeled as uncorrelated Rayleigh fading and we consider either MR and ZF schemes. Under these circumstances, the SE is derived in closed-form expressions with the aid of the MMSE channel estimation. Furthermore, it is possible to say that a SE is considered achievable when the probability of error belonging to a given transmitted signal goes to zero as the message length tends to infinity [9].

C. Downlink Data Transmission

The DL data transmission involves the BSs applying a linear precoding technique over the data signal, before sending it towards their respective UEs. Then, BS l realizes the following precoding process:

$$\mathbf{x}_l = \sum_{k=1}^{K}\mathbf{w}_{lk}\varsigma_{lk}, \quad (11)$$

where $\varsigma_{lk} \sim \mathcal{N}_{\mathbb{C}}(0,1)$ is the message signal with respect to UE k within cell l and $\mathbf{w}_{lk} \in \mathbb{C}^M$ indicates the transmit precoding vector of UE k within BS l with a unit norm, $\|\mathbf{w}_{lk}\|^2 = 1$.

By concluding the precoding process, the BS j sends the precoded signals to respective UEs, wherein the UE k receives:

$$\mathbf{y}_{jk} = \sqrt{\rho^{\mathrm{dl}}}\sum_{l=1}^{L}\sum_{k=1}^{K}\mathbf{g}^{\mathrm{T}}_{jlk}\mathbf{x}_l + \mathbf{n}_j, \quad (12)$$

where ρ^{dl} is the normalized DL transmit power. Note the presence of a transpose operator on the channel vector, owing

[4]The term "effective" indicates that the interfering signal are treated judiciously as an additional source of noise.

$$\gamma_{jk}^{\mathrm{mr,ul}} = \frac{M\rho^{\mathrm{ul}}\psi_{jjk}}{1+\rho^{\mathrm{ul}}\sum_{l=1}^{L}\sum_{k=1}^{K}\beta_{jlk}+M\rho^{\mathrm{ul}}\sum_{l=1,l\neq j}^{L}\psi_{jlk}} \tag{9}$$

$$\gamma_{jk}^{\mathrm{zf,ul}} = \frac{(M-K)\rho^{\mathrm{ul}}\psi_{jjk}}{1+\rho^{\mathrm{ul}}\sum_{l=1}^{L}\sum_{k=1}^{K}(\beta_{jlk}-\psi_{jlk})+(M-K)\rho^{\mathrm{ul}}\sum_{l=1,l\neq j}^{L}\psi_{jlk}} \tag{10}$$

to the considered reciprocity between UL and DL phases. From the above equation, it is also possible to see that the precoding associated with one UE is affected by the precoding vectors of the whole system. This fact turns the selection of precoding vectors a hard problem to be solved.

Nonetheless, influenced by the UL-DL duality, we adopt the MR and ZF precoding techniques as the solution of the transmit precoding problem. In this way, the message-bearing is focused in the direction of a UE of interest by the application of [3]:

$$\mathbf{w}_{jk} = \begin{cases} \frac{1}{\sqrt{M}}\hat{\mathbf{g}}_{jjk}^{*} & \text{, Maximum Ratio} \\ \sqrt{M-K}\hat{\mathbf{g}}_{jjk}^{*}\left(\hat{\mathbf{g}}_{jjk}^{\mathrm{T}}\hat{\mathbf{g}}_{jjk}^{*}\right)^{-1} & \text{, Zero-Forcing} \end{cases}. \tag{13}$$

Like the UL case, the DL achievable SE is acquired through an equivalent of the use-and-forget technique, as applied in [5]. That being said, the DL SE is:

$$\mathrm{SE}_{jk}^{\mathrm{dl}} = \frac{1}{2}\left(1-\frac{\tau_{\mathrm{p}}}{\tau_{\mathrm{c}}}\right)\log_2\left(1+\gamma_{jk}^{\mathrm{dl}}\right) \tag{14}$$

where $\gamma_{jk}^{\mathrm{dl}}$ is the DL effective SINR which depends on all precoding vectors within or outside cell j. The effective SINR for the MR and ZF is correspondingly given by (15) and (16).

D. Analyzing the Effective SINR Expressions

Observing the expressions acquired for the $\gamma_{jk}^{\mathrm{ul}}$ and $\gamma_{jk}^{\mathrm{dl}}$, we can promptly see that they are frequency-independent, since only second order statistics remain. Such result is a straight consequence of the massive number of antennas, the lower bound technique applied (use-and-forget) and, indirectly, the channel hardening effect. In the numerator, we observe a gain which is proportional to M for MR and $M-K$ for ZF. The reduction for ZF is expected and it is a consequence of the null-placement of the signals in order to avoid the intra-cell interference. Herein, we will nominate this last gain as the coherent beamforming or array gain, where the term "coherent" is a reference to the proportional dependence with M [5]. The effective strength of the received signals is given by $\rho^{\mathrm{ul}}\psi_{jjk}$ and $\rho^{\mathrm{dl}}\psi_{jjk}$. Notice that if the channel was perfectly known in BS, then ψ_{jjk} would be equal to β_{jjk} achieving the maximum possible strength.

The denominator is comprised of the undesired effects and can be disassembled into three components: the first right-handed is the receiver noise term consisted of the white Gaussian noise variance "1"; the second, a non-coherent interference which arises in account of the intra-cell and inter-cell disturbances, being this quantity proportional to the average large-scale coefficient for MR and to the mean variance of the estimation error for ZF. In the DL, this value is even proportional to K, due to the transmitted signal be a summation over all precoded data; the third term represents a coherent inter-cell interference being directly a consequence of the pilot contaminating UEs. One should bear in mind that the latter will increase together with the coherent beamforming gain when M goes large.

It is important to emphasize that the array gain acquired for the UL and DL is coming from distinct sources. Firstly for the UL, the BS receives M different observations of the desired signal sent from a UE, and then, they are coherently added. Thus, the power of the received signal increases proportionally to M, while the noise realizations add incoherently owing to its independence [9]. For the DL, the M degrees of freedom provide M distinct paths to a signal transmitted from a BS and received by a UE. Therefore, the signal power for each antenna is reduced by a factor of $1/M$ or looking at the magnitude $1/\sqrt{M}$. Then, the precoder add up coherently the M signals on the UE side. Ergo, the resultant signal has a magnitude of $M/\sqrt{M}$, whereby the power shows a tendency to be proportional with M.

III. Numerical Results

The performance of the home cell employing a classical M-MIMO system is investigated along this section. It is considered a dense urban multi-cell scenario, as shown in Fig. 1. There are seven hexagon cells[5], each one with a radius of 500 m. The BSs are equipped with M = 100 antennas and each of them is serving K = 18 single-antenna UEs that are uniformly distributed within the cell area.

TABLE I
Simulation parameters for dense urban scenario [5].

Parameter	**Value**
Carrier frequency	1.9 GHz
Spectral bandwidth	20 MHz
Coherence bandwidth (B_{c})	200 kHz
Coherence time (T_{c})	1 ms
Coherence interval (τ_{c})	200 samples
Pilot length (τ_{p})	K
Noise variance	-90.99 dBm
Radiated power per terminal	200 mW
Total radiated power per BS	200 mW
Monte Carlo Realizations	1000

The average large-scale coefficient is simply modeled as

$$\beta_{jlk} = \frac{\xi_{jlk}}{d_{jlk}^{\kappa}}, \tag{17}$$

[5]The hexagon is used, since it is the closest shape to a circle that permits a good representation of non-overlapping cells involving the coverage area of a macro-cell BS [5].

$$\gamma_{jk}^{\mathrm{mr,dl}} = \frac{M\rho^{\mathrm{dl}}\psi_{jjk}}{1 + K\rho^{\mathrm{dl}}\sum_{l=1}^{L}\sum_{k=1}^{K}\beta_{jlk} + M\rho^{\mathrm{dl}}\sum_{l=1,l\neq j}^{L}\psi_{jlk}} \tag{15}$$

$$\gamma_{jk}^{\mathrm{zf,dl}} = \frac{(M-K)\rho^{\mathrm{dl}}\psi_{jjk}}{1 + K\rho^{\mathrm{dl}}\sum_{l=1}^{L}\sum_{k=1}^{K}(\beta_{jlk} - \psi_{jlk}) + (M-K)\rho^{\mathrm{dl}}\sum_{l=1,l\neq j}^{L}\psi_{jlk}} \tag{16}$$

where ξ_{jlk} is the log-normally distributed shadow-fading, i.e., $10\log_{10}(\xi_{jlk}) \sim \mathcal{N}(0, \sigma^2_{\mathrm{shad.}})$, being $\sigma_{\mathrm{shad.}}$ its standard deviation. Moreover, d_{jlk} is the distance from UE k within cell l to BS j and κ is the decay or pathloss exponent. In our simulations, we have adopted $\sigma_{\mathrm{shad.}}$ = 8 dB and κ = 3.76, while the others parameters were described in Tab. I.

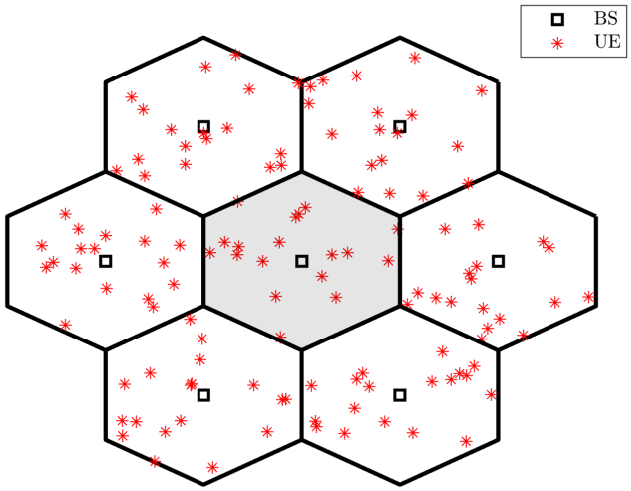

Fig. 1. Snapshot of a dense urban multi-cell setup with L = 7 cells and K = 18 UEs. The pilots are reused across the cells and they are assigned randomly. The shaded cell at the center represents the home cell, wherein the operation performance is being evaluated.

A. Uplink Pilots and Channel Estimation

The estimation performance will be evaluated via the mean-squared error (MSE), which is defined based on the Bayesian approach [10]. Thus, the normalized mean-square error (NMSE) in (18) expresses a relative amount of error obtained in the estimation of the channel vectors within the home cell (hc). Equivalently, the expression in (19) corresponds to the estimation error computed for the channel estimates from the neighboring cells (nc) in relation to BS j . Note that those quantities are random variables due to the UEs positions and the shadowing fading. In such expressions, also notice that $\beta_{jjk} - \psi_{jjk}$ is the average variance of the estimation error given by $\frac{1}{M}\mathrm{tr}\left((\beta_{jjk} - \psi_{jjk})\mathbf{I}_M\right)$, as well as occurs for the average large-scale coefficient.

$$\mathrm{NMSE}_j^{\mathrm{hc}} \triangleq 10\log_{10}\left(\frac{1}{K}\sum_{k=1}^{K}\frac{\beta_{jjk} - \psi_{jjk}}{\beta_{jjk}}\right) \tag{18}$$

$$\mathrm{NMSE}_{jl}^{\mathrm{nc}} \triangleq 10\log_{10}\left(\frac{1}{LK}\sum_{l=1,l\neq j}^{L}\sum_{k=1}^{K}\frac{\beta_{jlk} - \psi_{jjk}}{\beta_{jlk}}\right) \tag{19}$$

Fig. 2 shows the estimation performance based on the above metrics as a function of the radiated power per UE, being this quantity proportional to the signal-to-noise ratio (SNR). The estimation for a single-cell systea good form to observe the effect of pilot contamination is to obtain its averam was plotted as a baseline, whereby solely the home cell is considered to operate. Following the intuition, when the power increases, the estimation error is expected to decrease. However, observe that the multi-cell lines achieve a stable floor for a power approximately equals to 2 mW, whereas the single-cell curve decreases without any bound. This is a straight consequence of the pilot reuse across the cells, where it originates an effective noise floor in the estimate, as can be seen in (3). Also, note that the difference of the two multi-cell plots stems from the power gap between the UEs located at the home cell and those situated at the surrounding cells; supposing that the home cell's UEs commonly have a smaller pathloss than the UEs attached to surrounding cells. At last, we emphasize that the MSE is not the best metric to quantify the pilot contamination[6], since the MSE can not differ the interference from the noise. However, it is possible to see the pilot contamination presence through the given curves.

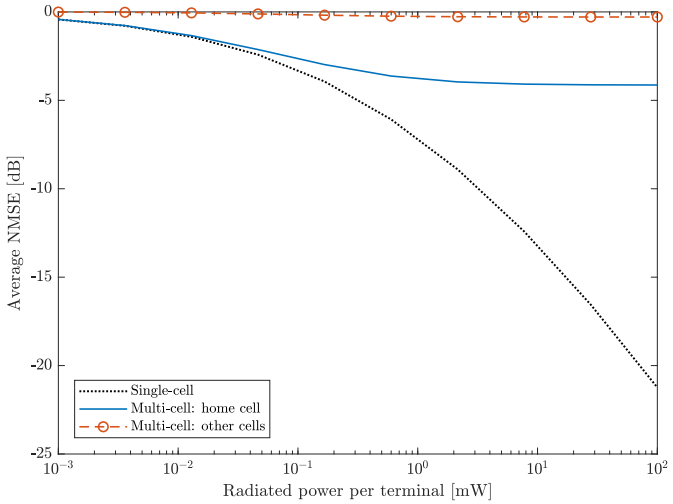

Fig. 2. Average normalized MSE as a function of the UL radiated power, which is proportional to the SNR ratio.

B. Uplink Spectral Efficiency

1) Varying M: The average UL SE is demonstrated in Fig. 3 as a function of M in a logarithmic scale. The MR and ZF combining techniques are applied in the multi-cell scenario, as well as in the single-cell context, as previously presented. It is evident that the single-cell curves increase without any

[6]For instance, ge level in comparison to the signal power.

limit, i.e., put more antennas on the BS is always beneficial to enhance the data rate. It is also clear that the SE for single-cell has a linear increase trend with M in a logarithmic scale. Another expected result with ease of visualization is a better performance of the ZF in relation to the MR, where the latter suffers additionally with the intra-cell interference and the channel non-orthogonality. Nonetheless, recall that the MR is more computationally simple. In sum, it can be inferred that the multi-cell case performs poorly, because of the coherent and non-coherent interferences that arise from the impact of pilot contamination and the operation of other cells.

Interestingly, one observes that the SE curves are a monotonically increasing function of M, however, the multi-cell case has a much smaller growth rate than the single-cell counterpart. This can be explained due to the fact that the coherent beamforming and the coherent interference in the multi-cell case are growing in an identical proportion with M. Then, it is possible to conclude that increasing M does not provide an adequate improvement of the SE, where not even one order-of-magnitude was achieved for the multi-cell scenario. This can be mathematically seen by the fact that M is inside the logarithm in (8). To summarize, the SE gains assigned with SINR enhancements, as the increment of M or even ρ^{ul}, only give moderate results. Therefore, they are not a good solution to obtain the desired data rates promised to be operating in the upcoming 5G.

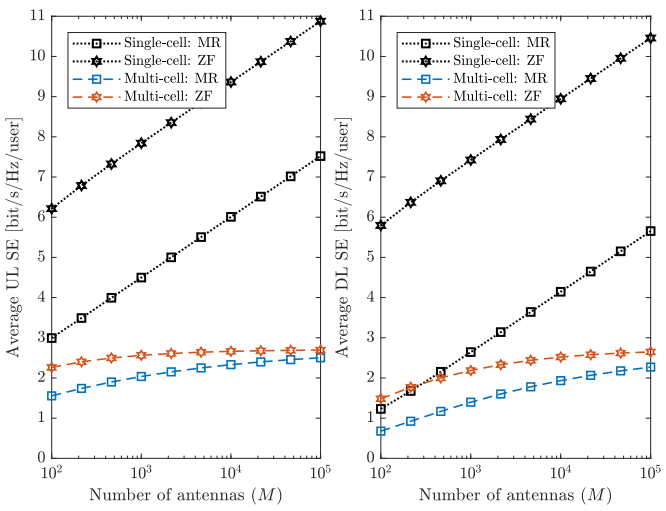

Fig. 3. Average SE per UE versus M for UL and DL; adopting $K = 18$. The total radiated power per terminal is the same to per BS and it is equals to 200 mW.

2) Varying K: The improvement of the SINR just achieves logarithmic gains for the SE. In view of this, it is desirable to rise the SE applying a procedure that entails an operation outside of the logarithm. This can be fortunately done through the usage of SDMA, which functionality embraces the spatial multiplexing of the UEs. Therefore, the sum SE increases with the summation of K SEs, which is the so-called multiplexing gain. However, it is easy to see that the growth of K directs to more interference over the communication, as shown in (9) and (10) for the UL. Attempting to combat this undesirable effect, M and K are mutually increased to balance an M/K (antenna-UE) ratio. Notice that the increase of M opposes to the interferences generated by the UEs. These commented behaviors are exemplified in Fig. 4, where the average sum UL SE was plotted as a function of K for both receive combining schemes and for two values of M: 10 and 100. The curves are in line with the results reported in [8], [9]. One can heed that the growing rate of the sum SE achieved in the $M = 100$ scenario is better than the provided by $M = 10$; taking into account that the antenna-UE ratio for the former is greater than for the latter.

For ZF, we can note that when $M = K$, all the degrees of freedom are spent exhaustively in the inter-cell interference combat and hence no array gain is provided. Also, one observes that all the curves presented in the graph tends to begin at zero, where any UE is multiplexed, and to end either at zero, when $K = 200$. This is expected due to the fact that τ_{c} will be equals to τ_{p} for the last case, and then, the pre-log factor in (8) is going to be zero. Notice that this is a direct consequence of the use of orthogonal pilots within each cell. Moreover, it is possible to say that, although the sum SE increases more than one order-of-magnitude because of SDMA, the SE per UE is not significantly increased.

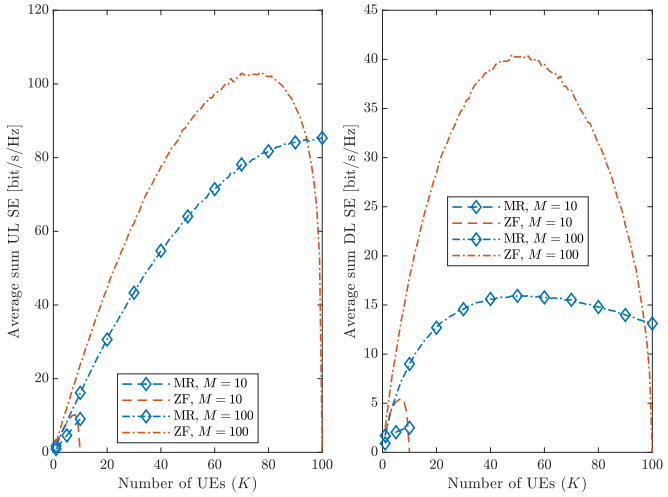

Fig. 4. Average sum SE versus K for UL and DL; adopting $M = 100$. The total radiated power per terminal is the same to per BS and it is equals to 200 mW.

C. Downlink Spectral Efficiency

1) Varying M: Fig. 3 shows the average DL SE varying with M. Note that the achievable SE in DL is slight lesser than the UL SE, as a consequence of the former secures a non-coherent interference proportional to K^2. The other conclusions made for the UL case, also hold for the DL.

2) Varying K: The multiplexing gain provided for the SDMA is also acquired for the DL, as shown in Fig. 4. Some quantitative differences between the UL and DL are a consequence of the distinction presented on the SINR expressions and on the interference sources. Furthermore, the parabola shape for the ZF is a direct result of the fact that the non-coherent term is proportional to K^2. Due to the MR be extremely impacted by the non-coherent interference, it

is possible to conclude that the ZF case for DL achieves a better performance than the MR. Recall from (15) and (16) that β_{jlk} is multiplied by K^2 in MR, while in ZF we have $K^2(\beta_{jlk} - \psi_{jlk})$.

IV. Conclusions

Based on illustrative results, it was possible to demonstrate how a canonical M-MIMO system works by evaluating the channel estimation and payload data transmission phases. The given closed-form expressions and the comparison between single-cell and multi-cell cases contributed to a profound insight of the impact caused by pilot contamination. Moreover, the SE assessments are duly exemplified. In fact, it was discussed how we can achieve a reasonable gain in the SE of several orders-of-magnitude through the enhancements provided jointly by SDMA and the large number of BS antennas, i.e., maintaining a good antenna-UE ratio.

References

[1] J. G. Andrews, S. Buzzi, W. Choi, S. Hanly, A. Lozano, A. C. K. Soong, and J. C. Zhang, "What Will 5G Be?" *IEEE Journal on Selected Areas in Communications*, vol. 32, no. 6, pp. 1065–1082, 2014. [Online]. Available: http://arxiv.org/abs/1405.2957

[2] T. L. Marzetta, "Noncooperative cellular wireless with unlimited numbers of base station antennas," *IEEE Transactions on Wireless Communications*, vol. 9, no. 11, pp. 3590–3600, 2010.

[3] J. Hoydis, S. Ten Brink, and M. Debbah, "Massive MIMO in the UL/DL of cellular networks: How many antennas do we need?" *IEEE Journal on Selected Areas in Communications*, vol. 31, no. 2, pp. 160–171, 2013.

[4] E. G. Larsson, O. Edfors, F. Tufvesson, and T. L. Marzetta, "Massive MIMO for Next Generation Wireless Systems," *IEEE Communications Magazine*, vol. 52, no. 2, pp. 186–195, 2014.

[5] T. L. Marzetta, E. G. Larsson, H. Yang, and H. Q. Ngo, *Fundamentals of Massive MIMO*. Cambridge University Press, 2016.

[6] J. Vieira, S. Malkowsky, K. Nieman, Z. Miers, N. Kundargi, L. Liu, I. Wong, V. Owall, O. Edfors, and F. Tufvesson, "A flexible 100-antenna testbed for Massive MIMO," *2014 IEEE Globecom Workshops, GC Wkshps 2014*, pp. 287–293, 2014.

[7] H. Q. Ngo and E. G. Larsson, "No Downlink Pilots Are Needed in TDD Massive MIMO," *IEEE Transactions on Wireless Communications*, vol. 16, no. 5, pp. 2921–2935, 2017.

[8] E. Björnson, E. G. Larsson, and T. L. Marzetta, "Massive MIMO: Ten myths and one critical question," *IEEE Communications Magazine*, vol. 54, no. 2, pp. 114–123, 2016.

[9] E. Björnson, J. Hoydis, and L. Sanguinetti, *Massive MIMO Networks: Spectral, Energy, and Hardware Efficiency*. Now Publishers, 2018, vol. 11.

[10] S. M. Kay, *Fundamentals of Statistical Signal Processing: Estimation Theory*. Prentice Hall, 1993.

Appendix B – An Evaluation of Successive Pilot Decontamination in Massive MIMO

This paper has been removed due to copyright reasons. You can access it by the following link:

http://www.uel.br/revistas/uel/index.php/semexatas/article/view/34450/24955

Simulation code is also available on:

https://github.com/victorcroisfelt/eval-suc-pilot-decon-mmimo

Appendix C – Exponential Spatial Correlation with Large-Scale Variations in Massive MIMO Channel Estimation

This paper has been removed due to copyright reasons. You can access it by the following link:

https://doi.org/10.1002/ett.3563

Simulation code is also available on:

https://github.com/victorcroisfelt/exp-lsf-spatial-corr-mmimo-chn-est

Appendix D – Kaczmarz Precoding and Detection for Massive MIMO Systems

This paper has been removed due to copyright reasons. This article was accepted and presented in Marrakech, Morocco at the IEEE Wireless Communications and Networking Conference (WCNC) in April 2019. Publication is expected soon.